

EXPLORING SUPERSYMMETRY AT LINEAR COLLIDERS* **

JAN KALINOWSKI

Institute of Theoretical Physics, Warsaw University
Hoża 69, 00-681 Warszawa, Poland

(Received November 6, 2003)

At prospective $e^{\pm}e^{-}$ linear colliders (LC), supersymmetric particles can be produced copiously. Large production cross-sections of kinematically accessible sparticles and clean signatures will allow for very precise measurements of their masses and couplings and the determination of their quantum numbers. We discuss some methods and expected accuracies in determining low-energy parameters of the supersymmetric model from the high-precision LC data and from combined results of LC and LHC. Evolving the parameters from the low-energy scale to the high-scale, the fundamental supersymmetry parameters can be reconstructed to reveal the origin of supersymmetry breaking.

PACS numbers: 11.30.Er, 12.60.Jv, 13.10.+q

1. Introduction

Despite the lack of direct experimental evidence the idea of symmetry between bosons and fermions [1] is so attractive that the supersymmetric extension of the Standard Model is widely considered as one of the most natural scenarios. Exact supersymmetry (SUSY) does not introduce any new parameters and the Minimal Supersymmetric Standard Model with conserved R -parity (MSSM) is fully predictive — each known particle of the Standard Model (SM) has its supersymmetric partner which differs by spin $1/2$, and which couples with the strength equal to the corresponding SM coupling. Unfortunately, the predictability of the MSSM is lost because supersymmetry must be broken and the construction of a viable mechanism of SUSY breaking turns out to be a difficult issue. Since a realistic breaking scenario

* Presented at the XXVII International Conference of Theoretical Physics, “Matter to the Deepest”, Ustroń, Poland, September 15–21, 2003.

** Supported in part by the Polish State Committee for Scientific Research (KBN) grant 2 P03B 040 24 (2003–2005).

with the particle content of the MSSM cannot be constructed, a “hidden sector” is invoked where SUSY breaking is assumed to take place. Many models have been proposed along these lines: gravity-mediated, gauge-mediated, anomaly-mediated, gaugino-mediated *etc.* Variants of each model are characterized by a few parameters (usually defined at a high scale) leading to different phenomenological consequences.

From the phenomenological point of view the breaking of SUSY can be parameterized by the most general explicit breaking terms in the Lagrangian. Demanding gauge symmetry and stability against radiative corrections from higher scales, the soft-breaking terms are limited to [2]

$$(i) \text{ mass terms for the bino } \tilde{B}, \text{ wino } \tilde{W}^j [j = 1-3] \text{ and gluino } \tilde{g}^a [i = 1-8] \\ \frac{1}{2}M_1 \overline{\tilde{B}} \tilde{B} + \frac{1}{2}M_2 \overline{\tilde{W}}^i \tilde{W}^i + \frac{1}{2}M_3 \overline{\tilde{g}}^i \tilde{g}^i ,$$

$$(ii) \text{ trilinear } A_i \text{ and bilinear } B \text{ scalar couplings} \\ A_u H_2 \tilde{Q} \tilde{u}^c + A_d H_1 \tilde{Q} \tilde{d}^c + A_l H_1 \tilde{L} \tilde{l}^c - \mu B H_1 H_2 ,$$

$$(iii) \text{ and squark and slepton mass terms} \\ m_{\tilde{Q}}^2 (\tilde{u}_L^* \tilde{u}_L + \tilde{d}_L^* \tilde{d}_L) + m_{\tilde{u}}^2 \tilde{u}_R^* \tilde{u}_R + m_{\tilde{d}}^2 \tilde{d}_R^* \tilde{d}_R + \dots$$

If the above parameters are complex, new sources of CP violation are introduced. In total, the unconstrained low-energy MSSM has 105 parameters resulting in a rich spectroscopy of states and complex phenomenology of their interactions.

If the electroweak scale is not fine-tuned, the superpartner masses (at least some of them) need to be in the TeV range, and thus within the reach of present or next generation high-energy colliders. The Large Hadron Collider (LHC) will then certainly see SUSY. Many different characteristics from squark and gluino production and their subsequent decays will be explored and measured. In scenarios characterized by a handful of free parameters some of the elements of supersymmetry can be reconstructed [3].

However, to establish supersymmetry experimentally it will be necessary to accurately test the validity of supersymmetry relations, i.e. whether the quantum numbers and couplings of the superpartners agree with the corresponding parameters of the Standard Model. On the other hand, the pattern of supersymmetry breaking needs to be explored. Therefore it is important to determine the SUSY breaking parameters with high precision in order to reconstruct the underlying mechanism, which eventually involves extrapolations to high energy scales [4].

For all the above points an e^+e^- LC, like TESLA [5], would be an indispensable tool. Thanks to its unique features: clean environment, tunable

collision energy, high luminosity, polarized incoming beams, and additional e^-e^- , $e\gamma$ and $\gamma\gamma$ modes, the LC offers precise measurements¹ of masses, couplings, quantum numbers, mixing angles, CP phases *etc.* Therefore, the concurrent running of the LC and LHC (at least partial) is very much welcome [7]. In this case the LC would not only provide independent and precise checks of the LHC findings but could provide additional experimental input to the LHC analyses as well. Coherent analyses of data from the LHC *and* LC would allow for a much better, model independent reconstruction of low energy SUSY parameters. We will illustrate this point with one example of a joint analysis of the chargino/neutralino sectors. The interplay between LHC and LC is investigated in detail in the LHC/LC Study Group [8].

2. Reconstruction of low-energy SUSY parameters

In order to match the experimental accuracy, sufficiently precise and reliable theoretical predictions for the masses, coupling, production cross-sections, decay rates, asymmetries *etc.*, of the superpartners are required. Loop-corrections inevitably bring all SUSY breaking parameters into the analysis and at the end an overall global fit, like in the SM, to the data will be necessary. At tree-level, however, different sectors of the MSSM (*e.g.* sleptons, charginos or squarks, each with limited number of parameters) can be handled separately and analytically, providing a good starting point for the final fit. Therefore below we will

- ◇ start with charginos, which depend only on M_2 , μ , $\tan\beta$,
- ◇ add neutralinos, which depend in addition on M_1 ,
- ◇ include sleptons, which bring in $m_{\tilde{l}}$, A_l ,
- ◇ and finally squarks and gluinos, which introduce $m_{\tilde{q}}$, A_q and M_3 ,

to reconstruct at tree level the basic structure of SUSY Lagrangian.

In reality, even neglecting radiative corrections, it might be difficult to separate a specific sector since *e.g.* sleptons enter via t -channel in the chargino production processes, many production channels can simultaneously be open, other SUSY processes constitute an important background to SUSY process under study *etc.*

¹ Current experimental status of low-energy supersymmetry can be found in *e.g.* [6].

2.1. The chargino/neutralino sector

The mass matrix of the wino and charged higgsino, after the gauge symmetry breaking, is non-diagonal

$$\mathcal{M}_C = \begin{pmatrix} M_2 & \sqrt{2}m_W \cos \beta \\ \sqrt{2}m_W \sin \beta & |\mu|e^{i\Phi_\mu} \end{pmatrix}. \tag{1}$$

It is diagonalized by two unitary matrices acting on left- and right-chiral states [9] parameterized by two mixing angles $\Phi_{L,R}$ and three CP phases. The mass eigenstates, called charginos, are mixtures of wino and higgsino with the masses and mixing angles given by

$$m_{\tilde{\chi}_{1,2}^\pm}^2 = \frac{1}{2} [M_2^2 + |\mu|^2 + 2m_W^2 \mp \Delta], \tag{2}$$

$$\cos 2\Phi_{L,R} = -\frac{[M_2^2 - |\mu|^2 \mp 2m_W^2 \cos 2\beta]}{\Delta} \tag{3}$$

$$\Delta = [(M_2^2 - |\mu|^2)^2 + 4m_W^4 \cos^2 2\beta + 4m_W^2 (M_2^2 + |\mu|^2) + 8m_W^2 M_2 \Re(\mu) \sin 2\beta]^{1/2}.$$

The mass matrix of the $(\tilde{B}, \tilde{W}^3, \tilde{H}_1^0, \tilde{H}_2^0)$ is symmetric but non-diagonal

$$M_N = \begin{pmatrix} M_1 & 0 & -m_{ZC\beta SW} & m_{ZS\beta SW} \\ 0 & M_2 & m_{ZC\beta CW} & -m_{ZS\beta CW} \\ -m_{ZC\beta SW} & m_{ZC\beta CW} & 0 & -\mu \\ m_{ZS\beta SW} & -m_{ZS\beta CW} & -\mu & 0 \end{pmatrix}, \tag{4}$$

where $M_1 = |M_1| e^{i\Phi_1}$, $\mu = |\mu| e^{i\Phi_\mu}$. The mass eigenstates, neutralinos, are obtained by the 4×4 diagonalization matrix N , which is parameterized by 6 angles and 9 phases as [10]

$$N = \text{diag} \{ e^1, e^{i\alpha_1}, e^{i\alpha_2}, e^{i\alpha_3} \} R_{34} R_{24} R_{14} R_{23} R_{13} R_{12}, \tag{5}$$

where R_{jk} are 4×4 matrices describing 2-dim complex rotations in the $\{jk\}$ plane. CP is conserved in the neutralino sector if R_{jk} are real and $\alpha_i = 0 \pmod{\pi/2}$. The unitarity constraints on N can conveniently be formulated in terms of unitarity quadrangles built up by

- ◇ the links $N_{ik}N_{jk}^*$ connecting two rows i and j ,
- ◇ the links $N_{ki}N_{kj}^*$ connecting two columns i and j .

Unlike in the CKM or MNS cases of quark and lepton mixing, the orientation of all quadrangles is physical. In terms of quadrangles, CP is conserved

² Majorana phases $\alpha_i = \pm\pi/2$ describe different CP parities of the neutralino states.

if and only if all quadrangles have null area (collapse to lines or points) *and* are oriented along either real or imaginary axis. The imaginary parts of the complex parameters involved could most directly and unambiguously be determined by measuring suitable CP violating observables. However, thanks to the Majorana nature of neutralinos, a clear indication of non-zero CP violating phases in the chargino/neutralino sector can be provided by studying the energy behavior of the cross sections for non-diagonal neutralino pair production near thresholds [11], or invariant mass of neutralino decay products [12].

Recently an attempt to reconstruct M_1, M_2, μ and $\tan \beta$ has been undertaken [13] for a particular SUSY scenario, the SPS1a point, one of the CP-conserving Snowmass benchmark points (so-called ‘Snowmass Points and Slopes’) recommended for detailed SUSY studies [14]. In this scenario only the light chargino $\tilde{\chi}_1^\pm$ and two lightest neutralinos $\tilde{\chi}_1^0$ and $\tilde{\chi}_2^0$ can be explored at the initial phase of the LC with $\sqrt{s} \leq 500$ GeV. Nevertheless, the entire tree level structure of the gaugino/higgsino sector can be reconstructed in analytical form as follows [9, 10].

The SPS1a parameters relevant for charginos and neutralinos

$$M_1=99.13 \text{ GeV}, M_2=192.7 \text{ GeV}, \mu=352.4 \text{ GeV}, \tan \beta=10$$

are defined at the electroweak scale; the full set of parameters is given in [15]. The resulting chargino and neutralino masses, together with the slepton masses of the first generation, are given in Table I. Although the $\tilde{\chi}_1^0 \tilde{\chi}_3^0$ and $\tilde{\chi}_1^0 \tilde{\chi}_4^0$ pairs would in fact be kinematically accessible at $\sqrt{s} = 500$ GeV, the production rates are small and the heavy states $\tilde{\chi}_3^0$ and $\tilde{\chi}_4^0$ decay via cascades to many particles. Therefore we constrain our analysis to the light chargino/neutralino states.

TABLE I

Chargino, neutralino and slepton masses in SPS1a, and the simulated experimental errors at the LC (in units of GeV) [16, 17].

	$\tilde{\chi}_1^\pm$	$\tilde{\chi}_2^\pm$	$\tilde{\chi}_1^0$	$\tilde{\chi}_2^0$	$\tilde{\chi}_3^0$	$\tilde{\chi}_4^0$	\tilde{e}_R	\tilde{e}_L	$\tilde{\nu}_e$
m	176.03	378.5	96.17	176.6	358.8	377.87	143.0	202.1	186.0
δm	0.55		0.05	1.2			0.05	0.2	0.7

Experimentally the masses of supersymmetric particles can be measured precisely either by threshold scans or in continuum above the threshold [16, 17]. The results of recent simulations are shown in Table I where expected experimental errors are listed. The chargino mixing angles $\cos 2\Phi_{L,R}$

can be determined in a model independent way using polarized electron beams [9]. Since the polarized chargino production cross sections $\sigma_{L,R}^\pm$ are simple binomials of $\cos 2\Phi_{L,R}$, the contour lines are of second order in the $\{\cos 2\Phi_L, \cos 2\Phi_R\}$ plane. In drawing contours in Fig. 1, the uncertainties

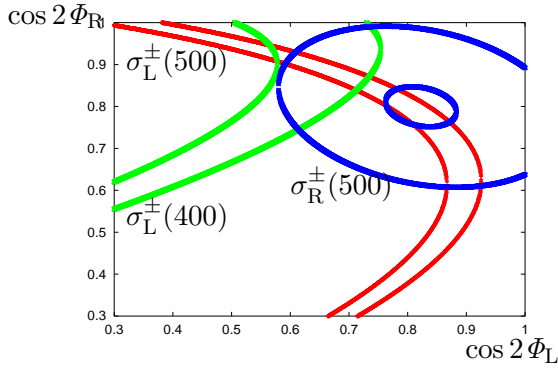


Fig. 1. Contours of the light chargino production cross sections with polarized electron beams at $\sqrt{s}= 400$ and 500 GeV in the plane $[\cos 2\phi_L, \cos 2\phi_R]$ [13].

due to the chargino mass error of $\delta m_{\tilde{\chi}_1^\pm} = 0.55$ GeV, sneutrino mass error of $\delta m_{\tilde{\nu}_e} = 0.7$ GeV, beam polarization error of $\delta P(e^\pm)/P(e^\pm) = 0.5\%$, and 1σ statistical error at 100 fb^{-1} have been included. We assume $P(e^+)=0.6$ and $P(e^-)=0.8$. The dominant error comes from $\delta m_{\tilde{\chi}_1^\pm}$; details of the analysis can be found in [13]. With the $\sqrt{s} = 500$ GeV data alone, two possible regions in the plane are selected. One of the regions can be removed with the help of the σ_L^\pm measured at $\sqrt{s} = 400$ GeV (σ_R^\pm is small and does not provide further constraints) resulting in the limited range

$$\cos 2\Phi_L = [0.62, 0.72], \quad \cos 2\Phi_R = [0.87, 0.91]. \tag{6}$$

In the CP conserving case, like the SPS1a, the constraint $|\cos \Phi_\mu| = 1$ allows us to solve Eqs. (2), (3) for M_2, μ and $\tan \beta$ in terms of the light chargino mass $m_{\tilde{\chi}_1^\pm}$ and mixing angles $\cos 2\Phi_L, \cos 2\Phi_R$ [9]. Defining

$$p = \pm \left| \frac{\sin 2\Phi_L + \sin 2\Phi_R}{\cos 2\Phi_L - \cos 2\Phi_R} \right|, \quad q = \frac{1 \cos 2\Phi_L + \cos 2\Phi_R}{p \cos 2\Phi_L - \cos 2\Phi_R}, \tag{7}$$

the SUSY parameters are determined as follows ($r^2 = m_{\tilde{\chi}_1^\pm}^2/m_W^2$):

$$M_2 = \frac{m_W}{\sqrt{2}} [(p + q) \sin \beta - (p - q) \cos \beta], \tag{8}$$

$$\mu = \frac{m_W}{\sqrt{2}} [(p - q) \sin \beta - (p + q) \cos \beta], \quad (9)$$

$$\tan \beta = \left[\frac{p^2 - q^2 \pm \sqrt{r^2(p^2 + q^2 + 2 - r^2)}}{(\sqrt{1 + p^2} - \sqrt{1 + q^2})^2 - 2r^2} \right]^\eta, \quad (10)$$

where $\eta = 1$ for $\cos 2\Phi_R > \cos 2\Phi_L$, and $\eta = -1$ otherwise. The relative signs of $\sin 2\Phi_L$, $\sin 2\Phi_R$ cannot be determined from CP-even $\tilde{\chi}_1^+ \tilde{\chi}_1^-$ cross sections and both possibilities in Eq. (7) have to be considered. Since $\tan \beta$ is invariant under simultaneous change of the signs of p, q , the definition $M_2 > 0$ can be exploited to remove this overall sign ambiguity. The parameters M_2, μ are then uniquely fixed if $\tan \beta$ is chosen properly. However, with the experimental precision of $\delta m_{\tilde{\chi}_1^\pm} = 0.55$ GeV and $\cos 2\Phi_L$ and $\cos 2\Phi_R$ in the ranges as given in Eq. (6), from Eqs. (8)–(10) one finds that M_2 is reconstructed within 10 GeV, μ within 40 GeV, and essentially no limit on $\tan \beta$ is obtained (only $\tan \beta > 6$). The main reason for this result is a relatively large error of the light chargino mass measurement.

So far we have exploited chargino sector alone. Now we will consider the neutralino sector to improve constrains on M_2, μ and $\tan \beta$ and, at the same time, to determine M_1 . As observables we include $m_{\tilde{\chi}_1^0}, m_{\tilde{\chi}_2^0}$ and cross sections $\sigma_{L,R}^0\{12\}$ and $\sigma_{L,R}^0\{22\}$ for production of $\tilde{\chi}_1^0 \tilde{\chi}_2^0$ and $\tilde{\chi}_2^0 \tilde{\chi}_2^0$ neutralino pairs measured at 400 and 500 GeV with polarized beams³.

We perform a simple $\Delta\chi^2$ test defined as

$$\Delta\chi^2 = \sum_i \left| \frac{O_i - \bar{O}_i}{\delta O_i} \right|^2. \quad (11)$$

The sum over physical observables O_i includes quantities listed above, \bar{O}_i stands for the physical observables taken at the input values of all parameters, and δO_i are the corresponding errors. Errors on neutralino masses are given in Table I. For the neutralino production cross sections the uncertainties due to statistics and experimental errors on beam polarizations, $\delta m_{\tilde{\chi}_1^\pm}, \delta m_{\tilde{e}_L}$ and $\delta m_{\tilde{e}_R}$ are included in the corresponding error δO_i ; details of error estimates can be found in [13]. The $\Delta\chi^2$ is then a function of unknown $M_1, \cos 2\Phi_L, \cos 2\Phi_R$ with $\cos 2\Phi_L, \cos 2\Phi_R$ restricted to the ranges given in Eq. (6), as predetermined from the chargino sector.

The left panel of Fig. 2 shows the contour of $\Delta\chi^2 = 1$ in the $\{M_1, \cos 2\Phi_L, \cos 2\Phi_R\}$ parameter space as derived from the LC data. The projection of the contour onto the axes determines 1σ errors for each parameter. Values obtained for $M_1, \cos 2\Phi_L, \cos 2\Phi_R$ together with $m_{\tilde{\chi}_1^\pm}$ can be inverted

³ The lightest neutralino-pair production cannot be observed. Alternatively, one can try to exploit photon tagging in the reaction $e^+e^- \rightarrow \gamma \tilde{\chi}_1^0 \tilde{\chi}_1^0$ [18].

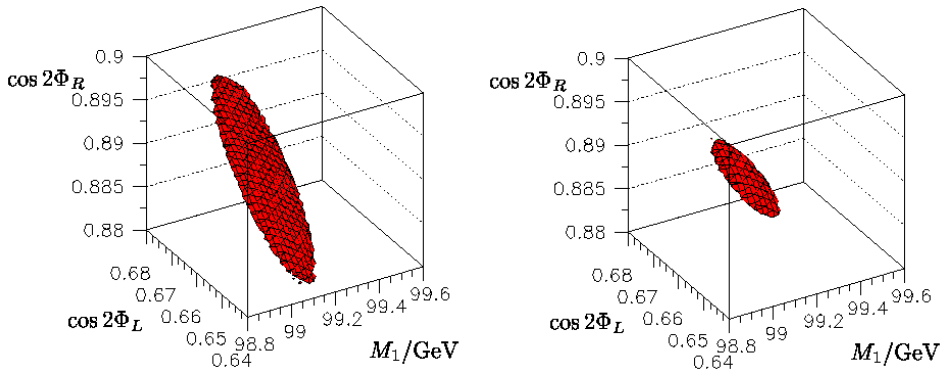


Fig. 2. The $\Delta\chi^2 = 1$ contour in the $\{M_1, \cos 2\Phi_L, \cos 2\Phi_R\}$ parameter space derived from the LC assuming $\mathcal{L} = 100 \text{ fb}^{-1}$ (left), and from the LC+LHC data (right) [13].

to derive M_2 , μ and $\tan\beta$. At the same time masses of heavy chargino $m_{\tilde{\chi}_2^\pm}$ and neutralinos $m_{\tilde{\chi}_3^0}$ and $m_{\tilde{\chi}_4^0}$ are predicted. As can be seen in Table II, the parameters M_1 and M_2 are determined at the level of a few per-mil, μ is reconstructed within a few per-cent and the error of $\leq 20\%$ for $\tan\beta$.

TABLE II

SUSY parameters with 1σ errors derived from the analysis of the LC data, and from the LC+LHC data. Shown are also the predictions for the heavier chargino/neutralino masses. Mass parameters are in GeV.

SUSY parameters			Mass predictions		
Input	Errors		Input	Errors	
	LC only	LC+LHC		LC only	LC+LHC
$M_1 = 99.1$	0.18	0.13	$m_{\tilde{\chi}_2^\pm} = 378.5$	7.8	2.0
$M_2 = 192.7$	0.60	0.32	$m_{\tilde{\chi}_3^0} = 358.8$	8.6	2.1
$\mu = 352.4$	8.9	2.1	$m_{\tilde{\chi}_4^0} = 377.9$	8.1	
$\tan\beta = 10$	1.8	0.8			

Note that the errors on predicted masses of heavy chargino/neutralinos, which in the SPS1a scenario are predominantly higgsinos, are strongly correlated with the error of μ . However, the LHC experiments will be able to measure the masses of several sparticles, as described in detail in [19]. In particular, the LHC will provide a first measurement of the masses of $\tilde{\chi}_1^0$, $\tilde{\chi}_2^0$ and $\tilde{\chi}_4^0$. The measurements of $\tilde{\chi}_2^0$ and $\tilde{\chi}_4^0$ are achieved through the study

of the processes:

$$\tilde{\chi}_i^0 \rightarrow \tilde{\ell}\ell \rightarrow \ell\ell\tilde{\chi}_1^0, \quad i = 2, 4. \quad (12)$$

The invariant mass of the two leptons in the final state shows an abrupt edge, which can be expressed in terms of the masses of the relevant sparticles as

$$m_{l+l^-}^{\max} = m_{\tilde{\chi}_i^0} \left[\left(1 - \frac{m_{\tilde{\ell}}^2}{m_{\tilde{\chi}_i^0}^2} \right) \left(1 - \frac{m_{\tilde{\chi}_1^0}^2}{m_{\tilde{\ell}}^2} \right) \right]^{1/2}. \quad (13)$$

The uncertainty on the LHC measurement of $m_{\tilde{\chi}_2^0}$ and $m_{\tilde{\chi}_4^0}$ depends not only on the experimental error on the position of $m_{l+l^-}^{\max}$, but also on the uncertainty on $m_{\tilde{\chi}_1^0}$ and $m_{\tilde{\ell}}$. If the latter are taken from the LC, Table I, the precisions on the LHC+LC measurements of $m_{\tilde{\chi}_2^0}$ and $m_{\tilde{\chi}_4^0}$ become: $\delta m_{\tilde{\chi}_2^0} = 0.08$ GeV and $\delta m_{\tilde{\chi}_4^0} = 2.23$ GeV. Therefore, by providing in particular $m_{\tilde{\chi}_4^0}$ from end-point measurements [19], the LHC can considerably help to get a better accuracy on μ . The impact of including $m_{\tilde{\chi}_4^0}$ into the $\Delta\chi^2$ is shown in the right panel of Fig. 2, and the errors from the joint LC+LHC analysis are listed in Table II. The errors of μ and $\tan\beta$ from the LC analysis are considerably reduced once the measured mass $m_{\tilde{\chi}_4^0}$ at the LHC is taken into account, reaching a level where radiative corrections become relevant and which will have to be taken into account in future fits [20].

2.2. The sfermion sector

For the first and second generation sfermions the LR mixing is usually neglected. The slepton masses can be measured at a high luminosity LC collider by scanning the pair production near threshold. The production of smuons (and staus) proceeds via s -channel gauge-boson exchange, so that the sleptons are produced in a P -wave with a characteristic rise of the excitation curve $\sigma \propto \beta^3$, where $\beta = (1 - 4m_f^2/s)^{1/2}$ is the slepton velocity. Due to the exchange of Majorana neutralinos in the t -channel, selectrons can also be produced in S -wave ($\sigma \propto \beta$), namely for $\tilde{e}_R^\pm \tilde{e}_L^\mp$ pairs in e^+e^- annihilation and $\tilde{e}_R^- \tilde{e}_R^-, \tilde{e}_L^- \tilde{e}_L^-$ pairs in e^-e^- scattering. However, since the non-zero widths of the sleptons considerably affect the cross-sections near threshold, the effects beyond leading order in the theoretical predictions must be included [21]. This can be achieved in a gauge-invariant manner by shifting the slepton mass into the complex plane, $m_f^2 \rightarrow m_f^2 - im_f T_f$, in the full $2 \rightarrow 4$ matrix element for the production of off-shell sleptons and their subsequent decays. Moreover, the Coulomb re-scattering correction due to photon exchange between the slowly moving sleptons, beamstrahlung and ISR also play an important role.

Expectations for the R-selectron cross-sections at both collider modes are shown in Fig. 3 with the background from both the SM and MSSM sources, reduced by appropriate cuts, included [21]. Using polarized e^+e^- beams and $\mathcal{L} = 50 \text{ fb}^{-1}$ a (highly correlated) 2-parameter fit gives $\delta m_{\tilde{e}_R} = 0.20 \text{ GeV}$ and $\delta \Gamma_{\tilde{e}_R} = 0.25 \text{ GeV}$; the resolution deteriorates by a factor of ~ 2 for $\tilde{\mu}_R \tilde{\mu}_R$ production. For $e_R^- e_R^- \rightarrow \tilde{e}_R \tilde{e}_R$ the gain in resolution is a factor ~ 4 with only a tenth of the luminosity, compared to e^+e^- beams.

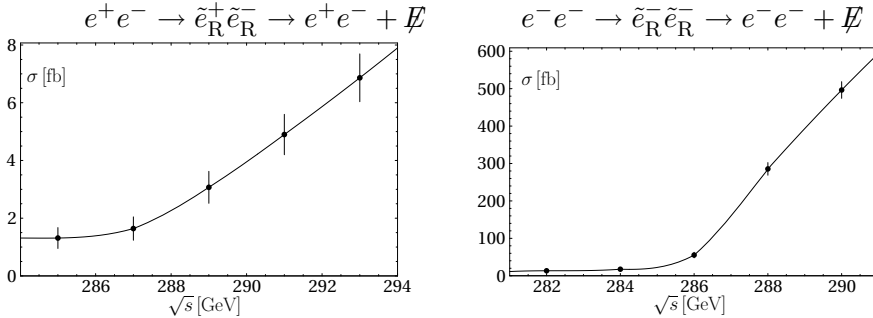


Fig. 3. Threshold excitation curves for \tilde{e}_R pair production. Errors for $\mathcal{L} = 10 \text{ fb}^{-1}$ in e^+e^- and 1 fb^{-1} in e^-e^- per scan point [21].

In contrast to the first two generations, large mixings are expected between the left- and right-chiral components of the third generation sfermions due to the large Yukawa coupling. The mixing effects are thus sensitive to the Higgs parameters μ and $\tan\beta$ as well as the trilinear couplings A_f .

The $\tilde{\tau}$ masses can be determined with the usual techniques of decay spectra or threshold scans at the per cent level, while the mixing angle $|\cos\theta_\tau|$ can be extracted with high accuracy from cross section measurements with different beam polarizations. A case study [22] at $\sqrt{s} = 500 \text{ GeV}$ with $\mathcal{L} = 250 \text{ fb}^{-1}$ shows that the following precision can be achieved: $m_{\tilde{\tau}_1} = 155 \pm 0.8 \text{ GeV}$, $\cos 2\theta_\tau = -0.987 \pm 0.08$.

If the higgsino component of the neutralino is sufficiently large, the polarization of τ 's from the $\tilde{\tau}_1 \rightarrow \tilde{\chi}_1^0 \tau$ decay turns out to be a sensitive function of $\tilde{\tau}$ mixing, neutralino mixing *and* $\tan\beta$ for high $\tan\beta$ [22, 23]. Simulations show that the τ polarization can be measured very accurately, $\delta P_\tau = 0.82 \pm 0.03$, which in turn allows to determine $\tan\beta = 20 \pm 2$, as shown in the left panel of Fig. 4. Moreover, if A_τ or μ turn out to be complex, the phase of the off-diagonal term $a_\tau m_\tau = (A_\tau - \mu^* \tan\beta) m_\tau = |a_\tau m_\tau| e^{iA_\tau}$ modifies $\tilde{\tau}$ properties, *e.g.* various $\tilde{\tau}$ decay branching ratios depend on the complex phases, see the right panel of Fig. 4. The fit to the simulated experimental data with 2 ab^{-1} gives an error of order 10% for $\Im m A_\tau$ and $\Re A_\tau$.

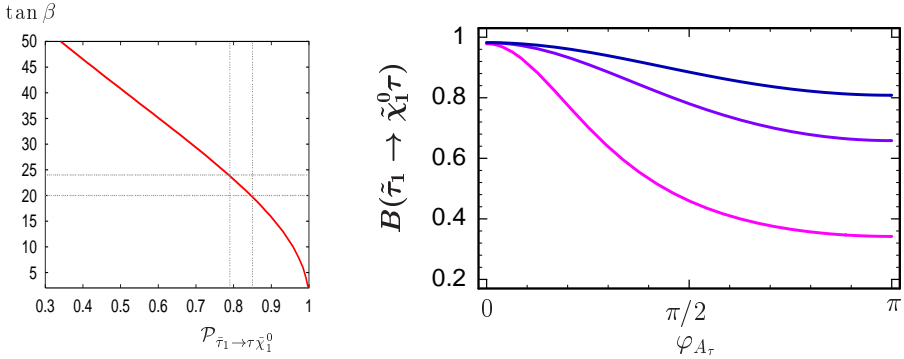


Fig. 4. Left: $\tan \beta$ as a function of τ polarization. From simulations $P_\tau = 0.82 \pm 0.03$ leading to $\tan \beta = 22 \pm 2$ [22]. Right: Branching ratios of $\tilde{\tau}_1$ as a function of φ_{A_τ} for $m_{\tilde{\nu}} = 233, 238, 243$ GeV (from bottom to top) [24].

Similarly, for the \tilde{t} and \tilde{b} sectors, the LR mixing can be important. By measuring the production cross sections with polarized beams the squark masses and mixing angles can be determined quite precisely, see the left panel of Fig. 5. Similarly to the $\tilde{\tau}$, the measurement of top quark polarization

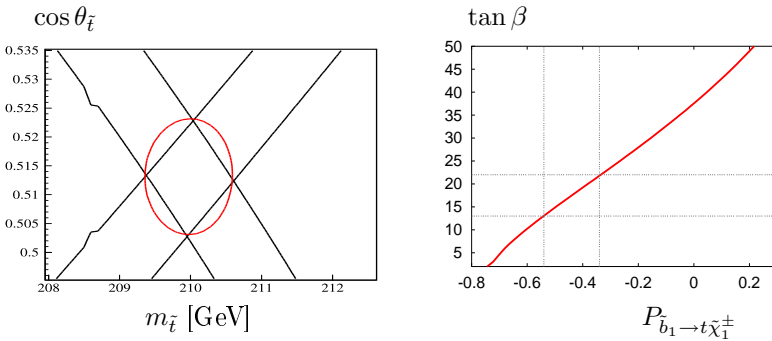


Fig. 5. Left: Contours of $\sigma_R(\tilde{t}_1 \tilde{t}_1)$ and $\sigma_L(\tilde{t}_1 \tilde{t}_1)$ as a function of $m_{\tilde{t}_1}$ and $\cos \theta_t$ for $\sqrt{s} = 500$ GeV, $\mathcal{L} = 2 \times 500$ fb $^{-1}$ [25]. Right: $\tan \beta$ as a function of top polarization. From simulations $P_t = -0.44 \pm 0.10$ leading to $\tan \beta = 17.5 \pm 4.5$ [22].

in the squark decay can provide information on $\tan \beta$. For this purpose the decay $\tilde{b}_1 \rightarrow t \tilde{\chi}_1^\pm$ is far more useful than $\tilde{t}_1 \rightarrow t \tilde{\chi}_k^0$ since in the latter the t polarization depends on $1/\sin \beta$ and therefore is only weakly sensitive to large $\tan \beta$. A fit to the angular distribution $\cos \theta_s^*$, where θ_s^* is the angle between the \bar{s} quark and the primary \tilde{b}_1 in the top rest frame in the decay chain $e^+e^- \rightarrow \tilde{b}_1 + t \tilde{\chi}_1^- \rightarrow \tilde{b}_1 + bc\bar{s} \tilde{\chi}_1^-$, yields for the top quark polarization $P_t = -0.44 \pm 0.10$, consistent with the input $P_t^{\text{th}} = -0.38$. From such a

measurement one can derive $\tan\beta = 17.5 \pm 4.5$, as illustrated in the right panel of Fig. 5. After $\tan\beta$ is fixed, measurements of stop masses and mixing allows to determine the trilinear coupling A_t at the ten-percent level [22].

3. Extrapolating to high-energy scale

Why do we need high precision measurements of the low-energy SUSY breaking parameters? The low-energy SUSY particle physics is characterized by energy scales of order $\lesssim 1$ TeV. However, the roots for all the phenomena we will observe experimentally in this range may go up to energies near the Planck $\Lambda_{\text{PL}} \sim 10^{19}$ GeV or the grand unification [GUT] scale $\Lambda_{\text{GUT}} \sim 10^{16}$ GeV. Information on physics near the high scale may become available from the extrapolation of parameters measured with high precision at laboratory energies. Although extrapolations exploiting renormalization group techniques extend over 13 to 16 orders of magnitude, they can be carried out in a stable way in supersymmetric theories [4].

Such a procedure, very successful in providing the base for the grand unification hypothesis of the three electroweak and strong gauge couplings, has recently been applied [26] to the minimal supergravity model (mSUGRA), the gauge mediated supersymmetry breaking model (GMSB) and superstring effective field theories.

As an example, consider the mSUGRA scenario characterized by the universal gaugino mass $M_{1/2} = 250$ GeV, scalar mass $M_0 = 200$ GeV, trilinear coupling $A_0 = -100$ GeV, $\text{sign}(\mu) > 0$ (the modulus $|\mu|$ determined by radiative symmetry breaking) and $\tan\beta = 10$. This scenario is close to the SPS1a [14], except for the M_0 which was taken slightly larger for merely illustrative purpose. The parameters $M_{1/2}$, M_0 and A_0 are defined at the GUT scale M_U where gauge couplings unify $\alpha_i = \alpha_U$. The RGE are then used to determine the low-energy SUSY Lagrangian parameters.

Based on simulations and estimates of expected precision, the low-energy ‘experimental’ values listed in Table III are taken as the input for the evolution of the mass parameters in the bottom-up approach to the GUT scale. The results for the evolution of the mass parameters of the first two generations to the GUT scale M_U is shown in the left panel of Fig. 6. The accuracy deteriorates for the squark mass parameters and for the Higgs mass parameter $M_{H_2}^2$. The origin of the differences between the errors for slepton, squark and Higgs mass parameters can be traced back to the numerical size of the coefficients. The quality of the test is apparent from second column of Table III, where it is shown how well the reconstructed mass parameters at the GUT scale reproduce the input $M_{1/2} = 250$ GeV and $M_0 = 200$ GeV.

For comparison, the right panel of Fig. 6 shows the evolution of the mass parameters of the first two generations in the GMSB model SPS8.

TABLE III

Representative gaugino/scalar mass parameters and couplings as determined at the electroweak scale and evolved to the GUT scale in the mSUGRA scenario based on LHC and LC simulations; masses in GeV. The errors are 1σ [26].

	Exp. input	GUT value
M_1	102.31 ± 0.25	250.00 ± 0.33
M_2	192.24 ± 0.48	250.00 ± 0.52
M_3	586 ± 12	250.0 ± 5.3
μ	358.23 ± 0.28	355.6 ± 1.2
$M_{L_1}^2$	$(6.768 \pm 0.005) \times 10^4$	$(3.99 \pm 0.41) \times 10^4$
$M_{E_1}^2$	$(4.835 \pm 0.007) \times 10^4$	$(4.02 \pm 0.82) \times 10^4$
$M_{Q_1}^2$	$(3.27 \pm 0.08) \times 10^5$	$(3.9 \pm 1.5) \times 10^4$
$M_{U_1}^2$	$(3.05 \pm 0.11) \times 10^5$	$(3.9 \pm 1.9) \times 10^4$
$M_{D_1}^2$	$(3.05 \pm 0.11) \times 10^5$	$(4.0 \pm 1.9) \times 10^4$
$M_{H_1}^2$	$(6.21 \pm 0.08) \times 10^4$	$(4.01 \pm 0.54) \times 10^4$
$M_{H_2}^2$	$(-1.298 \pm 0.004) \times 10^5$	$(4.1 \pm 3.2) \times 10^4$
A_t	-446 ± 14	-100 ± 54
$\tan \beta$	9.9 ± 0.9	—

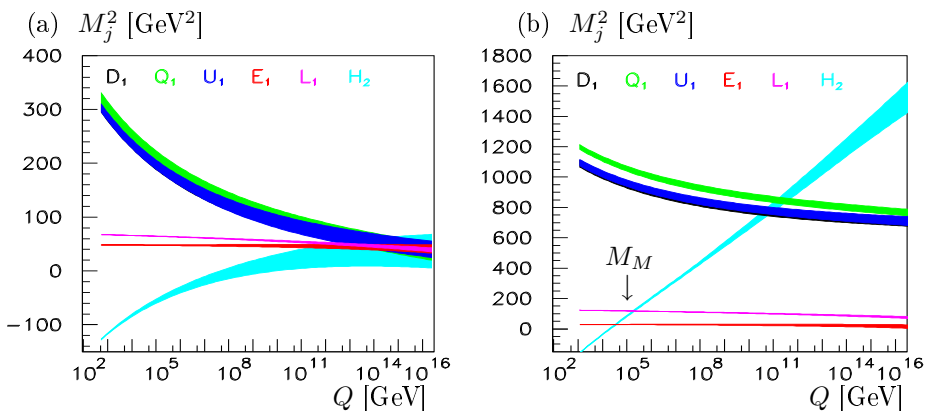


Fig. 6. Evolution, from low to high scales, of first-generation sfermion mass parameters squared and the Higgs mass parameter $M_{H_2}^2$ for (a) the mSUGRA point SPS1a, (b) the GMBS point SPS8. Widths of the bands indicate the 1σ CL [26].

The running of the scalar masses is quite different in both theories. The bands of the L -slepton M_L^2 and the Higgs $M_{H_2}^2$ parameters, which carry the same moduli of standard-model charges, cross at the scale M_M . The crossing, indicated by an arrow in Fig. 6, is a necessary condition for the GMSB scenario. Moreover, at the messenger scale M_M the ratios of scalar masses squared in the simplest version of GMSB are determined solely by group factors and gauge couplings, being independent of the specific GMSB characteristics.

This bottom-up approach, formulated by means of the renormalization group, makes use of the low-energy measurements to the maximum extent possible and it reveals the quality with which the fundamental theory at the high scale can be reconstructed in a transparent way. Therefore high-quality experimental data are necessary in this context, that should become available by future lepton colliders to reveal the fundamental theory at the high scale.

4. Summary and outlook

If low-energy supersymmetry is realized in nature, the LHC will provide plenty of data. However, their theoretical interpretation will be possible in specific models. In this context the e^+e^- linear collider will be an indispensable tool. Even a partial overlap of the LC running with the LHC would greatly help to perform critical tests: quantum numbers, masses, couplings *etc.* We have seen that from the future high-precision data taken at e^+e^- linear colliders, TESLA in particular, and combined with results from LHC, the low-energy parameters of the supersymmetric model can be determined. Then the bottom-up approach, by evolving the parameters from the low-energy scale to the high scale by means of renormalization group techniques, can be exploited to reconstruct the fundamental supersymmetry parameters at the high scale.

So far most analyses were based on lowest-order expressions. With higher-order corrections now available, one can attempt to refine the above program. In fact this is the goal of a new initiative, the SPA project [27], organized within the new ECFA Study of Physics and Detectors for a Linear Collider [28]. Many new theoretical calculations and future experimental analyses will be necessary. However, the temptation of revealing secrets of the ultimate unification of all interactions should provide a strong stimulus in this direction.

I would like to thank the Organizers of the Conference for their warm hospitality. I am grateful to K. Desch, G. Moortgat-Pick, U. Martyn, M. Nojiri, G. Polesello and P. Zerwas for many stimulating discussions.

REFERENCES

- [1] J. Wess, B. Zumino, *Nucl. Phys.* **B70**, 39 (1974); H.P. Nilles, *Phys. Rep.* **110**, 1 (1984); H.E. Haber, G.L. Kane, *Phys. Rep.* **117**, 75 (1985).
- [2] L. Girardello, M.T. Grisaru, *Nucl. Phys.* **B194**, 65 (1982).
- [3] F.E. Paige, [hep-ph/0211017](#); J.G. Branson, D. Denegri, I. Hinchliffe, F. Gianotti, F.E. Paige, P. Sphicas (eds.) [ATLAS and CMS Collaborations], *Eur. Phys. J. directC* **4**, N1 (2002).
- [4] E. Witten, *Nucl. Phys.* **B188**, 513 (1981).
- [5] E. Accomando *et al.*, ECFA/DESY LC Working Group, *Phys. Rep.* **299**, 1 (1998); TESLA Technical Design Report Part III: Physics at an e^+e^- Linear Collider, eds. R. Heuer, D.J. Miller, F. Richard, P.M. Zerwas, DESY 01-011 and [hep-ph/0106315](#).
- [6] A summary of current LC studies can be found *e.g.* in J. Kalinowski, [hep-ph/0309235](#), and references therein.
- [7] J. Kalinowski, [hep-ph/0212388](#).
- [8] The web address of the LHC/LC Study Group:
<http://www.ippp.dur.ac.uk/~georg/lhc1c/>.
- [9] S.Y. Choi, A. Djouadi, M. Guchait, J. Kalinowski, H.S. Song, P.M. Zerwas, *Eur. Phys. J.* **C14**, 535 (2000); S.Y. Choi, A. Djouadi, H.K. Dreiner, J. Kalinowski, P.M. Zerwas, *Eur. Phys. J.* **C7**, 123 (1999).
- [10] S.Y. Choi, J. Kalinowski, G. Moortgat-Pick, P.M. Zerwas, *Eur. Phys. J.* **C22**, 563 (2001); S.Y. Choi, J. Kalinowski, G. Moortgat-Pick, P.M. Zerwas, *Eur. Phys. J.* **C23**, 769 (2002); [hep-ph/0202039](#).
- [11] J. Kalinowski, *Acta Phys. Pol. B* **34**, 3441 (2003).
- [12] S.Y. Choi, [hep-ph/0308060](#).
- [13] K. Desch, J. Kalinowski, G. Moortgat-Pick, M.M. Nojiri, G. Polesello, SUSY Parameter Determination in Combined Analyses at LHC/LC, Proc. LHC/LC working group document, see [8].
- [14] B.C. Allanach *et al.*, *Eur. Phys. J.* **C25**, 113 (2002).
- [15] The values of benchmarks are listed on
<http://www.ippp.dur.ac.uk/~georg/sps>
- [16] H.U. Martyn, LC-note LC-PHSM-2003-071; M. Dima *et al.*, *Phys. Rev.* **D65**, 071701 (2002).
- [17] M. Ball, diploma thesis, University of Hamburg, January 2003; talk by K. Desch at the ECFA/DESY Linear Collider workshop, Prague, November 2002, <http://www-hep2.fzu.cz/ecfadesy/Talks/SUSY/>.
- [18] S. Ambrosanio, B. Mele, G. Montagna, O. Nicrosini, F. Piccinini, *Nucl. Phys.* **B478**, 46 (1996).
- [19] B.K. Gjelsten, E. Lytken, D. Miller, P. Osland, G. Polesello, contribution in the LHC/LC working group document, see [8].

- [20] S. Kiyoura, M.M. Nojiri, D.M. Pierce, Y. Yamada, *Phys. Rev.* **D58**, 075002 (1998); T. Blank, W. Hollik, [hep-ph/0011092](http://arxiv.org/abs/hep-ph/0011092); H. Eberl, M. Kincel, W. Majerotto, Y. Yamada, *Phys. Rev.* **D64**, 115013 (2001); T. Fritzsche, W. Hollik, *Eur. Phys. J.* **C24**, 619 (2002).
- [21] A. Freitas, D.J. Miller, P.M. Zerwas, *Eur. Phys. J.* **C21**, 361 (2001); A. Freitas, A. von Manteuffel, [hep-ph/0211105](http://arxiv.org/abs/hep-ph/0211105).
- [22] E. Boos *et al.*, *Eur. Phys. J.* **C30**, 395 (2003).
- [23] M.M. Nojiri, *Phys. Rev.* **D51**, 6281 (1995); M.M. Nojiri, K. Fujii, T. Tsukamoto, *Phys. Rev.* **D54**, 6756 (1996).
- [24] A. Bartl, K. Hidaka, T. Kernreiter, W. Porod, *Phys. Rev.* **D66**, 115009 (2002), LC-TH-2003-027.
- [25] A. Finch, H. Nowak, A. Sopczak, LC-PHSM-2003-075.
- [26] G.A. Blair, W. Porod, P.M. Zerwas, *Eur. Phys. J.* **C27**, 263 (2003).
- [27] The web address of the SPA project: <http://www-flc.desy.de/spa/>
- [28] The web address of the ECFA Study of Physics and Detectors for a Linear Collider: <http://www.desy.de/conferences/ecfa-lc-study.html>